City Research Online

City, University of London Institutional Repository

This is the accepted version of the paper.

This version of the publication may differ from the final published version.

Permanent repository link: https://openaccess.city.ac.uk/id/eprint/24754/

Link to published version:

City Research Online: http://openaccess.city.ac.uk/   publications@city.ac.uk

Finite element analysis and calculation method of residual flexural capacity of post-fire RC beams

Bin Cai[1,2] Bo Li[1] Feng Fu[2*]

Abstract: Fire tests and subsequent bending tests of four reinforced concrete (RC) beams were performed. Based on these tests, the post-fire performance of RC beams was further studied using finite element simulation through reasonable selection of suitable thermal and thermodynamic parameters of steel and concrete materials. A thermodynamic model of RC beams with three sides under fire was built using finite element analysis (FEA) software ABAQUS. The FEA model was validated with the results of fire tests. Different factors were taken into account for further parametric studies in fire using the proposed FE model. The results show that the main factors affecting the fire resistance of the beams are the thickness of the concrete cover, reinforcement ratio of longitudinal steel, the fire exposure time and the fire exposure sides. Based on the strength reduction formula at high temperature of steel and concrete, an improved section method was proposed to develop a calculation formula to calculate the flexural capacity of RC beams after fire. The theoretical calculation method proposed in this paper shows good agreement with FEA results, which can be used to calculate the flexural capacity of RC beams after fire.

Keywords: post-fire ; reinforced concrete beams ; finite element ; ABAQUS ; theoretical calculation

1. Introduction

Reinforced concrete (RC), as one of the major building materials of modern architectural structures, will form nonuniform temperature fields after exposure to fire (Shao et al. 2003; Cheng 2007). The thermal stress and expansion (Zhao 2014) due to fire will lead to stress redistribution of overall structures and reduction of structural flexural capacity or even the local structural destabilization, which further induce the collapse of overall structures and bring about massive losses to the possessions and life of humans (Ban 2008). Thus, the temperature fields should be

* Corresponding author: E-mail address: cenffu@yahoo.co.uk

2 School of Mathematics, Computer Science and Engineering, City, University of London, London, UK,Full list of author information is available at the end of the article

determined first for subsequent analysis of RC structures to understand the degradation in the mechanical properties and flexural capacity after exposure to fire, which are the keys to evaluate whether the RC structures can be used anymore (Tian 2002; Zeng 2006). So far, there is considerable research in the aspect of test and finite element analysis (FEA). Fu et al. (2015) studied how the fire surfaces of RC beams affected the temperature fields. Liao et al. (2013) designed the shear tests and a FEA method was proposed to calculate the shear flexural capacity among one room temperature and seven post-fire RC beams, which has the accepted accuracy. Sun et al. (2002) investigated the mechanical performances in the tensile region and the compressive region of beam sections at elevating temperature and after cooling. Shi and Guo (2000) tested the structural performances of RC beams at high temperature and presented the temperature distributions of beam sections, a coupling temperature-stress constitutive law of concrete and the main performances at different surfaces after fire exposure. Lu et al. (1993) studied the 1-, 2- and 3-surface fire exposure of 12 RC simply-supported beams, presented the bending moment-curvature relations in different temperature fields and computationally validated the load-deflection relations of RC beams. EI-Hawavy et al. (1997) investigated the mechanical behavior of post-fire RC beams in the shear zone by the method of test. Parthasarathi et al. (2019) carried out experimental research on 10 RC short columns at different temperatures, obtained the deflection, stiffness and variation of the specimen at high temperature, and compared the experimental results with the FEA results. The results were reasonably well. Kodur and Agrawal (2017) studied the fire response of RC beams caused by temperature-induced bond degradation and an FEA was developed. Fu (2016a) developed 3D FE modelling approach using ABAQUS. Fu (2020) developed a machine learning algorithm for fire safety design. Eamon and Jensen (2013) conducted a reliability analysis of RC columns subjected to fire, and various factors such as the fire type, load ratio, reinforcement ratio, concrete cover, concrete strength were considered in the analysis. Xu et al. (2015) conducted a fire endurance test of 6 high strength steel RC continuous T-beams and confirmed the feasibility of designing high strength steel RC continuous T-beams using plastic analysis. Hassan et al. (2019) designed an experiment to investigate the effect of different retrofitting techniques on the performance of concrete at different temperature on 31 beams. Chen et al. (2009) carried out experimental research on the mechanical properties of 9 full-size concrete columns. The results showed that with the increase of fire time, the residual flexural capacity decreases. Mathew and Joseph (2018) studied

the flexural behavior of fly ash geopolymer concrete beams at different temperature. The results showed that the deformation characteristic of geopolymer concrete beams is similar to that of the reinforced cement concrete beams at ambient temperature, but big difference noticed at high temperature. Di Capua and Mari (2007) proposed two models, the thermal model and the mechanical model, for calculating the RC beams exposed to fire, which were in good agreement with test results. Bratina et al. (2003) explored the post-fire nonlinear structural analysis of RC beams. In theory, Xiang et al. (2010) studied the calculation method of flexural capacity for fire-damaged RC bending members, Yu et al. (2005) studied the effects of different factors on the mechanical properties of concrete exposed to high temperature and proposed the equations of stress-strain relation for various concrete after high temperature. Hu et al. (2006) established estimation methods for the flexural capacity of slabs subjected to fire and axially loaded concrete square columns subjected to fire on four surfaces. Lie and Irwin (1993) described a method for the calculation of the fire resistance of RC columns with rectangular cross sections. Jiang et al. (2008) discussed the rectangle beam with single reinforcement, and proposed a method to calculate the residual capacity of the RC member.

Based on above research, it can be seen that, most scholars' research primarily focusses on the constitutive relationship of materials during or after fire, as well as the response analysis and damage assessment, and the flexural capacity of theoretical calculation of the post-fire RC beams is barely investigated. In addition, the major factor affecting the behavior of the RC beams in fire is not well investigated. The 500 °C isotherm method specified in Eurocode (BSI 2004) is the most widely used theoretical calculation method for the residual bearing capacity of RC beams after fire. The method is based on the assumption that concrete above 500 °C does not provide load-bearing capacity to members, while concrete within 500 °C is considered to maintain its initial values of strength and elastic modulus. However, this method is a rough calculation method cannot accurately evaluate the structures after fire. BS 5950: Part 8 (2003) specifies a calculation method of the fire resistance of members in bending which is called 'moment capacity method' or called "section method". It is used primarily for steel sections but concrete members. Therefore, RC beams fire tests and subsequent bending test were performed in , this paper, based on the test results and the existing moment capacity method, proposes a new theoretical calculation model using improved section

method to calculate the flexural capacity of the post-fire beams. The model first conducts heat transfer analysis to obtain the temperature field of the beam section, and then divides the beam section to small divisions and obtain the average temperature of each divisions. Finally, based on the relationship of material strength reduction formulas in fire, the flexural capacity can be accurately obtained for RC beam after fire. Compared with the 500 °C isotherm method, the advantage of this method is that it fully considers the changes of the temperature field and accurately considers the changes of the material strength caused by the temperature changes in each micro area, and the results obtained are more accurate. The accuracy of the theoretical calculation is validated through the comparison with simulation and test results, which offers a new way for the evaluation of post-fire RC structures. In addtion,a thermodynamic model of RC beams with three sides under fire was built using finite-element analysis (FEA) software ABAQUS. The FEA model was validated with the results of fire tests. Different factors were taken into account for further parametric studies in fire using the propsed FE model.

2. Research methodology

For evaluating post-fire residual flexural capacity of RC beams, three approaches are adopted: experiment investigate (fire tests and post-fire static load tests) of RC beams (stage 1), numerical analysis of RC beams on the basis of Finite Element software (stage 2) and finally, theoretical analysis of residual flexural capacity on the basis of improved section method (stage 3). A flow chart in Fig. 1 illustrates the three stages for evaluating residual strength of fire exposed RC beams.
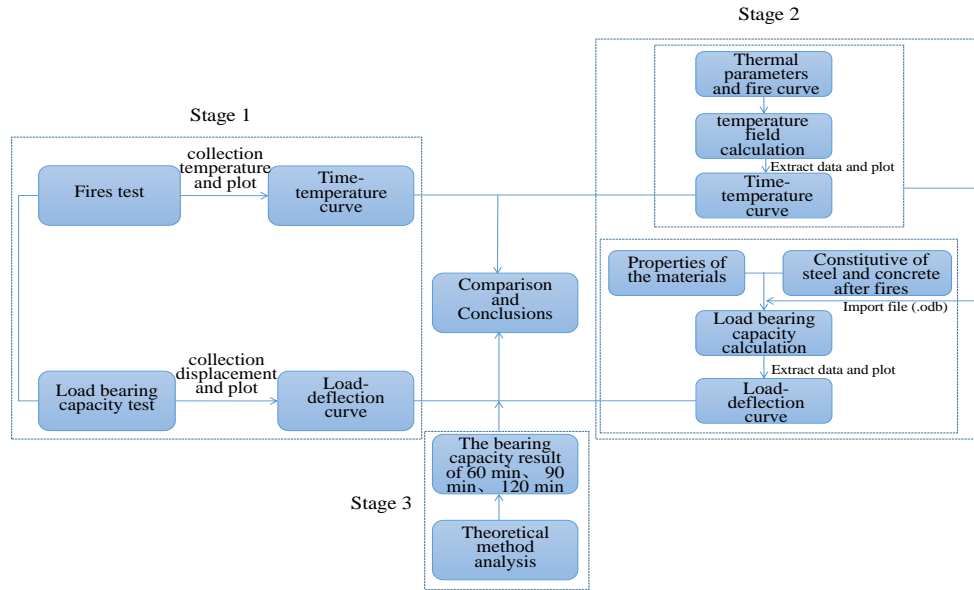
Fig. 1 Flow chart illustrating the three stages of RC beams exposed to fire

3. Fire and bending tests of RC beams

3.1 Fire tests

3.1.1 Test preparations

The experiments were conducted in the Structure Laboratory of Jilin Jianzhu University. 4 RC beams were fabricated with dimensions and reinforcement details shown in Fig. 2. The mix proportion of concrete (Table 1) is W:C:S:G=0.38:1:1.11:2.72. The basic parameters of the reinforcement are shown in Table 2. Two of them were exposed to 60 minutes high temperature in a furnace (Table 3). The temperature distribution of the beams subjected to fire were therefore obtained, which provides a comparison for the subsequent numerical analysis.

Table 1   Mix proportion of concrete

| Water (Kg)	Cement (Kg)	Sand (Kg)	Gravel (Kg)
175	461	512	1252

Table 2   Basic parameters of the reinforcement

Type of	Specification of	Yield strength	Ultimate strength	Elastic modulus

reinforcement	steels	(N/mm²)	(N/mm²)	(×10⁵N/mm²)
Pulled	HRB400	469	583	2.05
Compressed	HRB400	469	583	2.05
Stirrup	HPB300	346	431	2.13

Table 3　Basic parameters of specimens

Specimen No.	Concrete strength grade	Test conditions	Fire-exposure time (min)
N1	C30	Room-temperature static test	—
N2	C30	Room-temperature static test	—
F1	C30	Post-fire static test	60
F2	C30	Post-fire static test	60
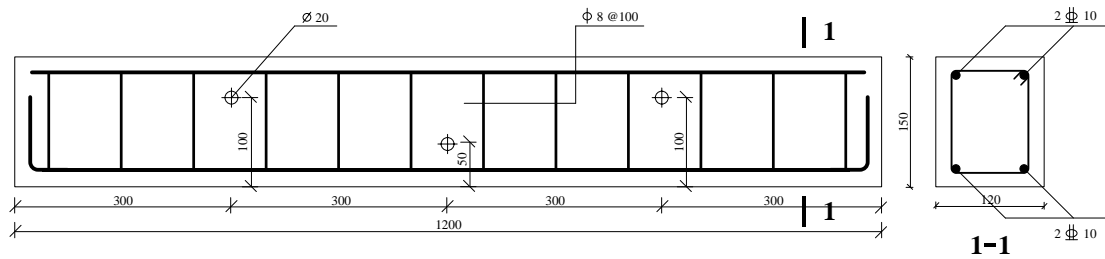
Fig. 2 Dimensions and reinforcement of beams

To record the temperature changes during the experiments, thermocouples were embedded into the pre-drilled holes of the beams F1 and F2 and filled with cement mortar. Then the beams were covered with fireproofing cotton at locations shown in Fig. 3 to simulate 3-sided fire exposure.

3.1.2 Test observations

The two beams were placed into a furnace (Fig. 4) for 60 minutes fire exposure. During the heating stage of the members, when the exposure time is 12 minutes, a small amount of water vapor

can be seen on the beam surface from the observation hole in the furnace. When the exposure time is 21 minutes, a large amount of water vapor volatilizes from the furnace, and the water vapor is the most vigorous when it is 27 minutes. As the exposure time increases, the water vapor in the furnace gradually decreases. When the exposure time is 42 minutes, the water vapor in the furnace basically disappears. The main reason for this phenomenon is that some of the free water inside the beam and the small amount of water gel evaporated at the beginning of the fire. As the temperature in the furnace increases, a large amount of free water and water gel begin to volatilize. At the same time, the beam is dehydrated in a large amount, and when the water vapor in the furnace is substantially disappeared, the beam is completely dehydrated.

When the RC beams are dehydrated at high temperature, the sound of slight cracking as well as a frequent slight popping can be heard. A large number of diagonal cracks are noticed on the surface of the beam when it is taken out from the furnace after tests, and the longer the exposure time is, the more larger the crack is. From the overall point of view, there are phenomena such as peeling, outer drum, and crispness, and the surface color changes from normal color to light yellow or even dark yellow. The reason for this phenomenon is that during the process of the fire, some complicated chemical reactions occur inside the beam, such as the decomposition of $Ca(OH)_2$ and minerals of aggregate, which cause certain damage to the interior of the beam. The internal expansion of the beam causes surface cracking.
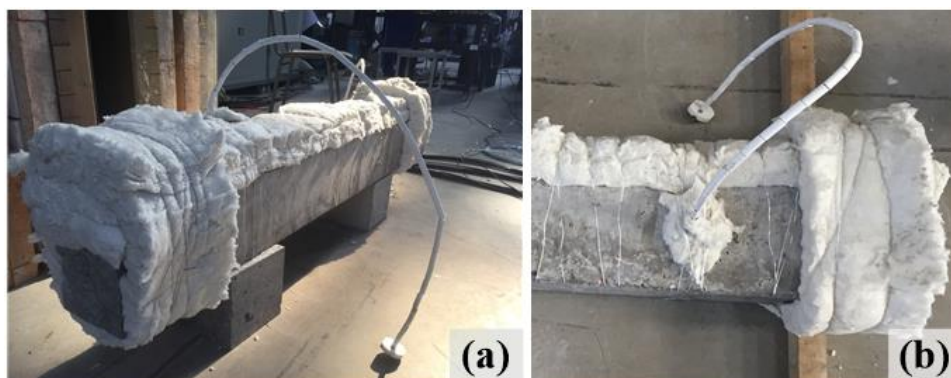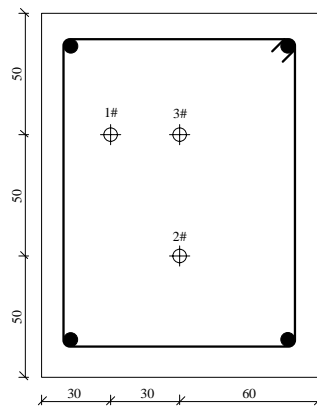

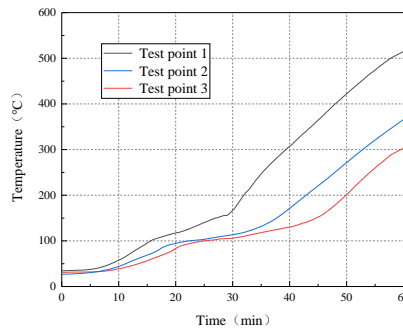**Fig. 3 Three-sided fire exposure and thermocouple layout**

Fig. 4 The equipment of high temperature furnace

Fig. 5 The temperature measuring points on the RC beams

Fig. 6 The time-temperature curves at different measuring points

3.1.3 Test results and analysis

Three temperature measuring points are set on each specimen (Fig. 5). The time-temperature curves (Fig. 6) of the three temperature measuring points of each beam section after 60 minutes of fire are obtained from the above beam tests. Due to the thermal inertia of concrete, the temperature distribution of the section is uneven after fire, and the temperature gradient is larger near the furnace. The temperature is generally rising, but it can be seen from the figure that there is a temperature platform at about 120 °C, which may due to the evaporation of water in the beam causing partial

heat loss.

3.2 Static tests

After fire tests, the two beams were cooled to room temperature, then, static tests were performed. The effects of fire exposure time on the flexural capacity of the beam were therefore, r investigated. In brief, 2 none-fire exposed beams and 2 post-fire beams were tested using a 4-point bending test rigs as it is shown in Fig. 7. The instrumentations are shown in Fig.7.

3.2.1 Test phenomena

Under the vertical load, the displacement of the RC beams gradually increases with the increase of the load. After a period of loading, tiny hairline cracks can be seen first in the mid-span of the beam. The crack l developed slowly and upward, and new vertical cracks appeared on both sides of the mid-span under the constant load. As the loading continued, the cracks gradually become longer, and the gaps become larger. After that, the displacement of the beam becomes larger and the load remained basically unchanged. After a while, the load drop rapidly, until the failure of the beam.
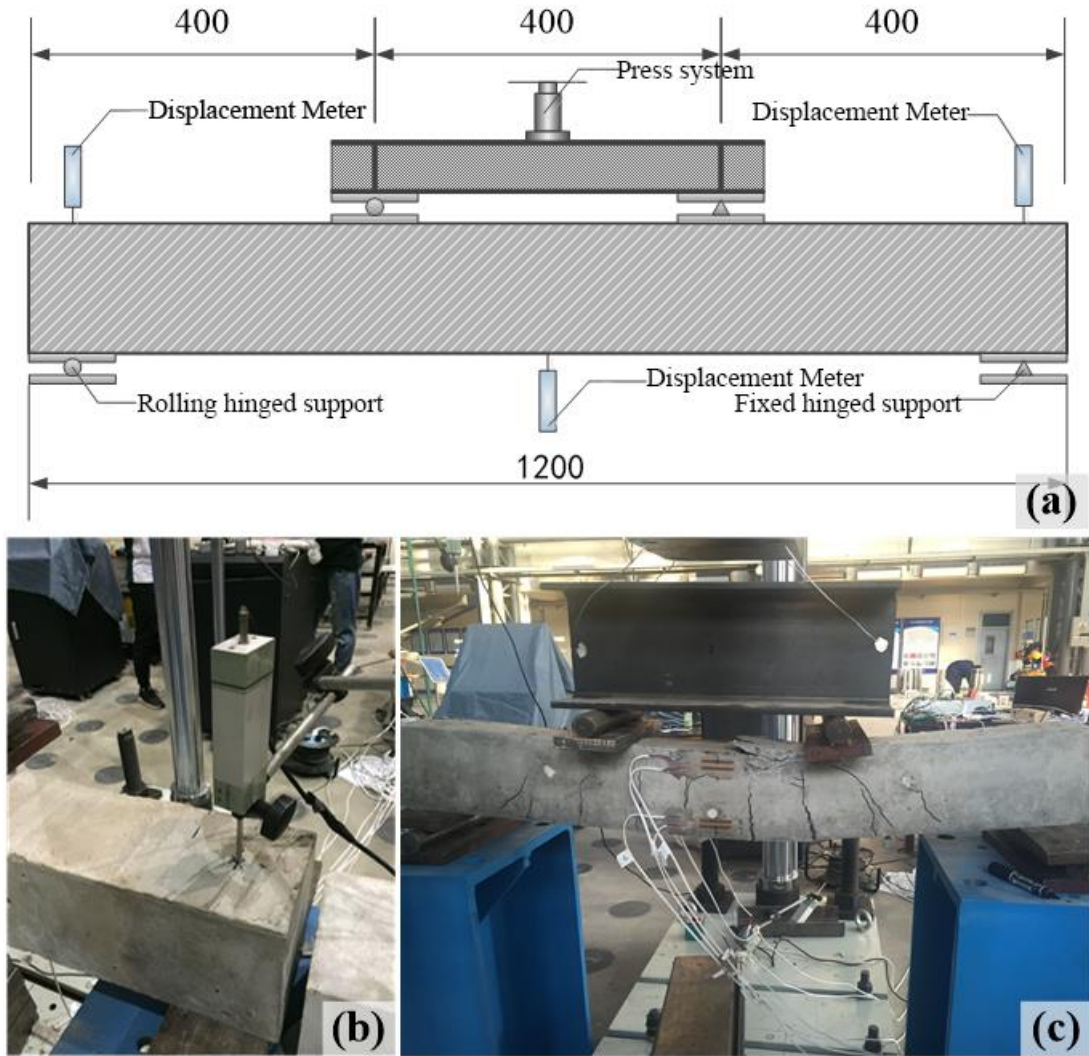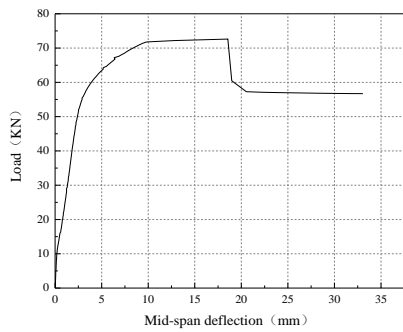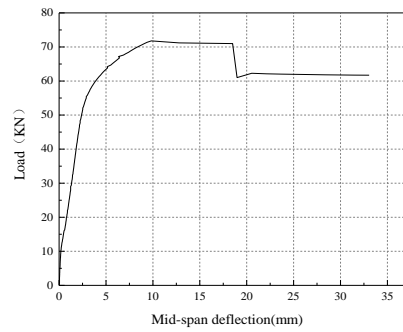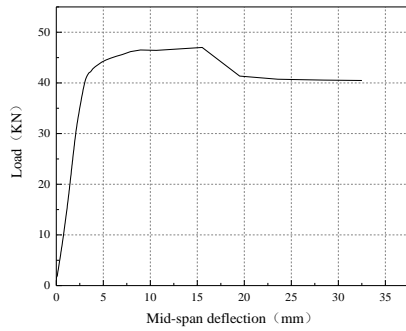
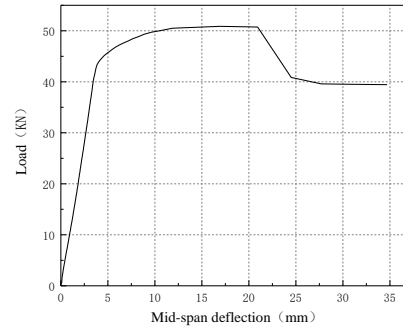**Fig. 7 Loading procedure**

（a） Beam N1

（b） Beam N2

(c) Beam F1　　　　　　　　　　　　(d) Beam F2

Fig. 8 Load-deflection curves of different beams

3.2.2 Test results and discussion

The load-deflection curves of the 4 beams were plotted in Fig. 8. Clearly, during the loading of the RC beams, the mid-span load-deflection relation first increased proportionally. When the load reached certain value, it did not increase any more, and the curve reached yield stage. Then the load dropped abruptly, and the beams failed. The curves showed the flexural capacity was weakened by about 30% after the fire exposure.

4. Finite element modelling

To be able to simulate the response of the RC beams after fire, a sequential Thermal-Mechanical Coupling approach is implemented in ABAQUS modelling. The heat transferring analysis was performed first to get the temperature distribution. The thermal result then input into the mechanical model for further mechanical analysis.

4.1 Basic assumptions

Some basic assumptions were proposed to simplify the simulation:

(1) The concrete strength of different mesh in the compression zone is different, but the strength in each mesh is regarded as a constant;

(2) The equivalent reduction coefficient of the concrete strength of the entire compression zone can be obtained by weighting the average of the cross-section compression zone area;

(3) The heat loss due to moisture evaporation during the fire was not considered;

(4) There was no bonding slip between the reinforcement and concrete.

4.2 Heat Transfer analysis
4.2.1 Thermal properties of the materials

To obtain temperature fields of RC beams, heat transfer analysis was performed using ABAQUS. The specific heat capacity, thermal conductivity, and density of the materials should be first determined, which are the basis for the analysis. The parameters were selected based on Wang and He (2009) .

The thermal conductivity of concrete λ_{cT} (W/(m·°C)) is:

$$\lambda_{cT} = 2 - 0.24\left(\frac{T}{120}\right) + 0.012\left(\frac{T}{120}\right)^2 \qquad (20°C \leq T \leq 1200°C) \tag{1}$$

where T is the temperature, °C.

The specific heat capacity of concrete C_{cT} (J/(Kg·°C)) is:

$$C_{cT} = 900 + 80\left(\frac{T}{120}\right) - 4\left(\frac{T}{120}\right)^2 \qquad (20°C \leq T \leq 1200°C) \tag{2}$$

The thermal conductivity of reinforcement steel λ_{sT} (W/(m·°C)) is:

$$\lambda_{sT} = \begin{cases} 54\text{-}3.33 \times 10^{-2}T & (20°C \leq T < 800°C) \\ 27.3 & (800°C \leq T \leq 1200°C) \end{cases} \tag{3}$$

The specific heat capacity of reinforcement C_{sT} (J/(Kg·°C)) is:

$$C_{sT} = \begin{cases} 425 + 7.73 \times 10^{-1}T - 1.69 \times 10^{-3}T^2 + 2.22 \times 10^{-6}T^3 & (20°C \leq T < 600°C) \\ 666 + \dfrac{13002}{738 - T} & (600°C \leq T < 735°C) \\ 545 + \dfrac{17820}{T - 731} & (735°C \leq T < 900°C) \\ 650 & (900°C \leq T \leq 1200°C) \end{cases} \tag{4}$$

4.2.2 Fire temperature curve

The heat transfer analysis was performed on the basis of a heating curve. Here the ISO-834 fire curve from the International Organization (ISO1999,) is adopted (Fig. 9). The curve can be expressed as (Fu 2016b,Fu 2018):

$$T = T_0 + 345 \lg(8t + 1) \tag{5}$$

where t is the heating time (min); T_0 is the initial room temperature (°C, which is 20 °C here).
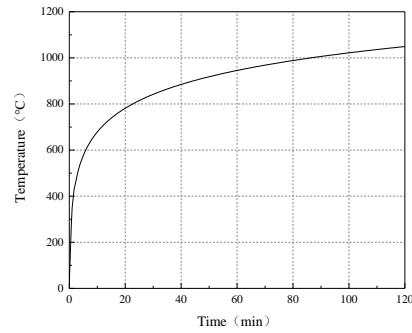
Fig. 9 The ISO-834 fire curve

4.2.3 FE model set up

A 3D finite element model is built as shown in Figure 10. The concrete was simulated as DC3D8 8-node (Fu,2010) linear heat transfer units, and the reinforcement steel as DC1D2 2-node heat transfer link units. The contact between reinforcement and concrete was simulated using Embedded Region The beams were exposed to fire on three sides, and the modes of heat transfer in the fire-exposed faces were surface radiation and surface film condition, and the unfired faces were surface film condition. The thermal parameters of the materials were calculated according to Eqs. (1) to (4). After the heat transfer analysis steps and boundary conditions were set up, the models were meshed into cells in size of 10 mm. The temperature distribution of RC beam exposed to fire is shown in Fig. 10, the temperature field nephogram (Fig. 11) and the simulated results (Fig. 12) were shown as follows.
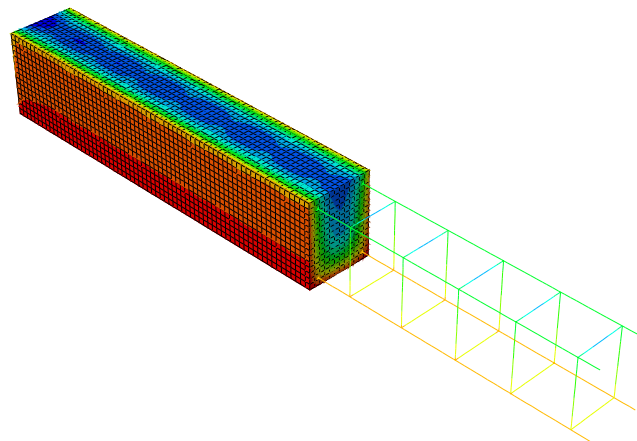
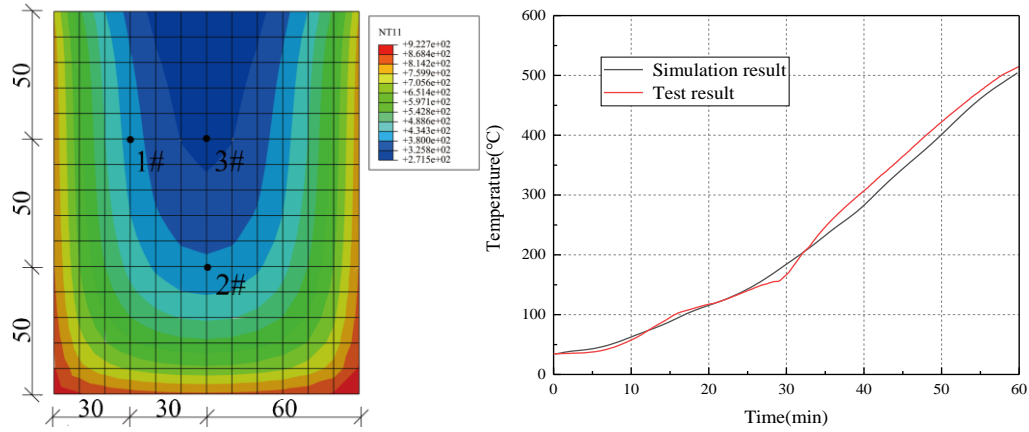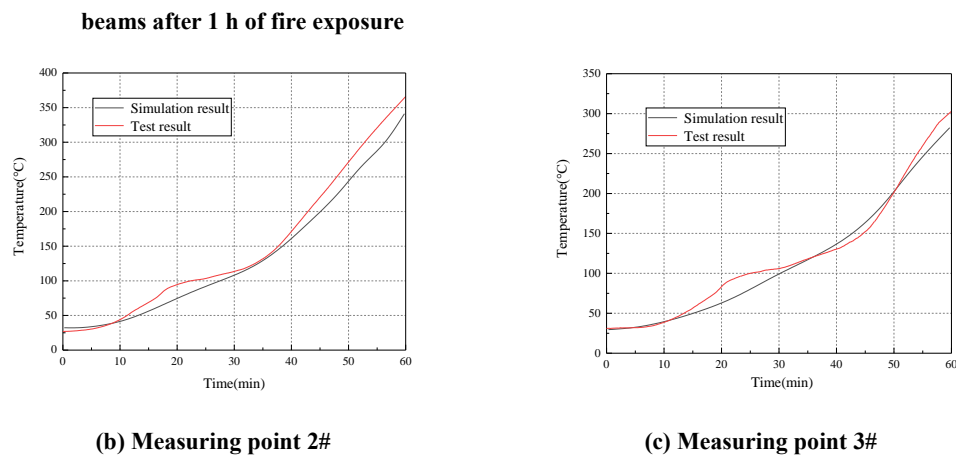**Fig. 10 The temperature field simulation of RC beam exposed to fire**

Fig. 11 Temperature field nephogram of the beams after 1 h of fire exposure

(a) Measuring point 1#

(b) Measuring point 2#

(c) Measuring point 3#

Fig. 12 Temperature measuring points and simulated results

4.2.4 FE model validation

The temperature fields of post-fire RC beams obtained using ABAQUS is compared with test results, which can be visually observed. The simulated results were basically consistent with the test results.

4.3 Static analysis procedure

The degradation of the compressive strength of concrete, the yield strength of steel at high temperature were related to the maximum temperature. In order to be consistent with the test conditions, the temperature field simulation was performed first to determine the strength degradation of the materials, then the static load simulation was carried out. The mechanical performances of reinforcement or concrete varied with the change of maximum temperature, so the relations with temperature should be considered to determine the post-fire mechanical performances.

They are determined according to the formula introduced in the following section.

4.3.1 Constitutive model of concrete under high temperature

The post-fire mechanical properties of concrete were related to the fire exposure time, way of cooling, and type of skeletal materials. Here the model of post-fire concrete proposed by Yu et al. (2005) was used. The compression stress-strain model (Fig. 13) of post-fire concrete can be determined according to formula 7 and 8. The reduction factor of axial compressive strength of concrete with temperature change was shown in Fig. 14 according to formula 6.

The strength reduction factor of post-fire concrete Ψ_{cT} at T °C is:

$$\Psi_{cT} = \frac{f_c(T)}{f_c} = \frac{1}{1 + 9 \times [(T-20)/800]^{c_1}} \tag{6}$$

where $f_c(T)$ is the axial compressive strength of concrete at high temperature, N/mm²; f_c is the axial compressive strength of concrete at room temperature, N/mm²; c_1 is the parameter. (which is 3.55 here for ordinary concrete), for high-performance concrete (HPC) concrete c_1=6.70.

The compression peak strain of post-fire concrete $\varepsilon_0(T)$ at T °C is:

$$\varepsilon_0(T) = \left\{1 + c_4[(T-20)/100]^2\right\}\varepsilon_0 \tag{7}$$

where ε_0 is the compressive strain of concrete at room temperature; c_4 is the parameter. (which is 0.037 here for ordinary concrete), for high-performance concrete (HPC) concrete c_4=0.017.

The compression stress-strain relationship of post-fire concrete can be expressed as:

$$y = \begin{cases} \dfrac{9.1 f_{cu}^{-4/9} x - x^2}{1 + (9.1 f_{cu}^{-4/9} - 2)x} & x \leq 1 \\[3mm] \dfrac{x}{2.5 \times 10^{-5} f_{cu}^3 (x-1)^2 + x} & x > 1 \end{cases} \tag{8}$$

where $y = \sigma_c/f_c(T)$, $x = \varepsilon_c/\varepsilon_0(T)$, σ_c is the compressive stress of post-fire concrete, N/mm²; ε_c is the compressive strain of post-fire concrete; f_{cu} is the cube crushing strength of concrete at room temperature, N/mm².
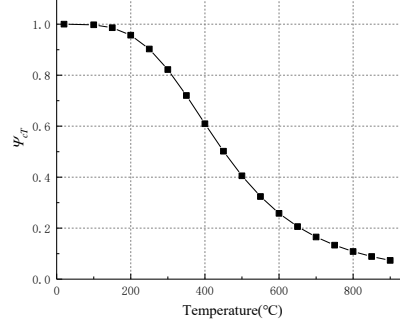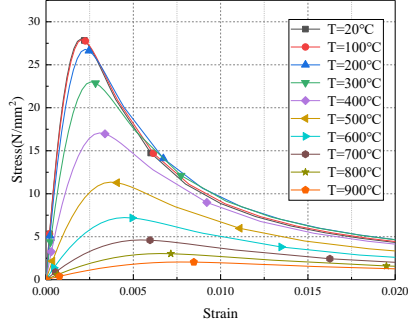
Fig. 13 The stress strain curves of concrete   Fig. 14 The reduction factor of concrete

at different temperature   compressive strength

The elastic modulus of post-fire concrete $E_c(T)$ (N/mm²) at T °C is:

$$E_c(T) = \frac{E_c}{1 + 2.15 \times 10^{-3}[(T-20)/800]^{4.33} + 3.7 \times 10^{-2}[(T-20)/100]^2}$$ (9)

where E_c is the elastic modulus of concrete at room temperature, N/mm².

The tensile strength of post-fire concrete was calculated by a bilinear model proposed by Hu et al. (2014).

The tensile strength of post-fire concrete $f_t(T)$ (N/mm²) at T °C is:

$$\frac{f_t(T)}{f_t} = 0.976 + \left[1.56 \times \left(\frac{T}{100}\right) - 4.35 \times \left(\frac{T}{100}\right)^2 + 0.345 \times \left(\frac{T}{100}\right)^3\right] \times 10^{-2} \qquad 20°C \leq T \leq 800°C$$ (10)

4.3.2 constitutive model of reinforcement at high temperature

The built-in bilinear kinematic reinforcement model of ABAQUS was used to simulate reinforcement steel, and the elastic modulus $E_s(T)$ (N/mm²) at T °C proposed by Yu et al. (2005) can be calculated as follows:

$$\frac{E_s(T)}{E_s} = \begin{cases} 1 & T \leq 350℃ \\ 1.0072 - 2.014 \times 10^{-7}T^2 + 5 \times 10^{-5}T & T > 350℃ \end{cases}$$ (11)

where E_s is the elastic modulus of reinforcement at room temperature, N/mm².

The yield strength reduction factor of reinforcement Ψ_{yT} at T °C proposed by Miao et al. (2013) is as follows:

$$\Psi_{yT} = \frac{f_y(T)}{f_y} = \begin{cases} 1 & 0℃ < T \leq 200℃ \\ 1.33 - 1.64 \times 10^{-3}T & 200℃ < T \leq 700℃ \end{cases}$$ (12)

where $f_y(T)$ is the post-fire yield strength of reinforcement , N/mm²; f_y is the yield strength of

reinforcement at room temperature, N/mm².

The stress-strain model of reinforcement at high temperature is shown as follows (Fig. 15).
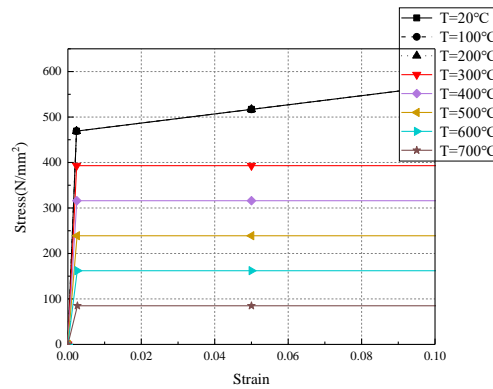
**Fig. 15 The stress-strain curves of steel at different temperature**

4.3.3 Modelling process

When the beams were simulated using ABAQUS, the constitutive relations of concrete and reinforcement under high temperature (as shown in Fig. 13 and Fig. 15) were input into the model. The contact between reinforcement and concrete was simulated through Embedded Region (Fu,2012,Fu,2008). The heat transfer analysis was first performed. Then the result file (.odb) of the heat transfer simulation results was imported into the predefined fields, the loads and analytical steps were followed. The mesh size was 10 mm, in which the concrete was set as C3D8R 8-node linear hexahedron units, while the reinforcement as T3D2 2-node linear 3-dimensional truss units. After submitted the job, the results were provided in Fig. 16. Finally, based on the post-processing function of the software, the post-fire load-deflection curves of the beams were plotted (Fig. 17).
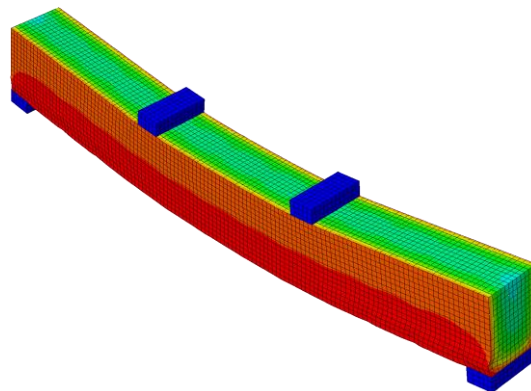
Fig. 16 The flexural capacity simulation of RC beam after fire

4.3.3 FE model validation

(a) at room temperature   **(b) after 1 h of fire exposure**
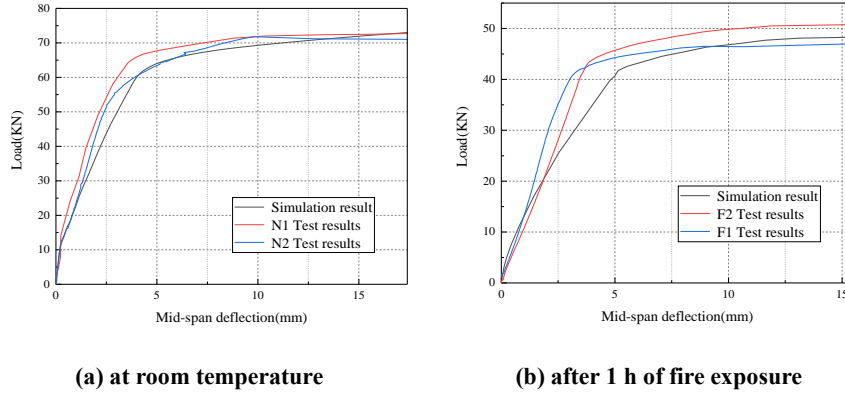
**Fig. 17 The tested and simulated load-deflection curves**

After RC beams was simulated in ABAQUS, the simulated and tested results of the post-fire flexural capacity of RC beams were compared, the simulated results were basically consistent with the test results.

5. Parametric analysis

The effects of concrete cover thickness (c), fire exposure time (t), the ratio of longitudinal reinforcement (ρ), the fire sides (n), and the ratio of shear span to effective depth (λ) on the post-fire load bearing ability were investigated using the validated model. Among them, the treatment of the cover thickness is achieved by fine-tuning (increasing 10mm and decreasing 10mm) the height of the beam section (h) on the basis of ensuring that the effective height (h_0) of the beam section remains unchanged. Thereby, the finite element analysis of these factors on the flexural capacity of RC beams can be clarified. The concrete cover thickness was 15, 25 or 35 mm; the fire exposure time was 60, 90 or 120 minutes; the longitudinal reinforcement ratio was 0.91%, 1.25% or 1.52%, the fire sides was 3 or 4, the ratio of shear span to effective depth was 2.2, 2.6, or 3.0. The analytical results were presented in Fig. 18. To study the effect of the thickness of the concrete cover, the height of the section is adjusted by fine-tuning (increasing and decreasing 10 mm) the cross-sectional dimensions of the beam to ensure that the effective height of the beam section remains unchanged.
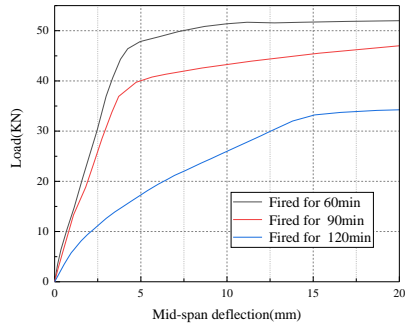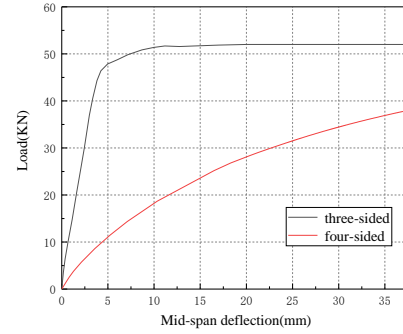
(a) load-deflection curves of
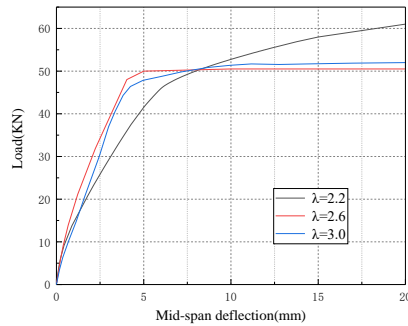
different fire exposure time
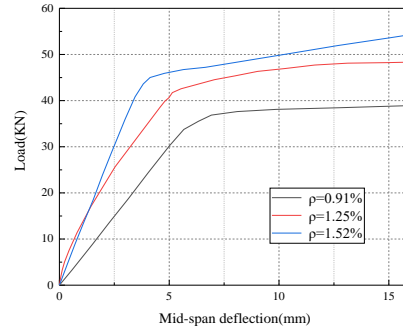
(b) load-deflection curves of

different reinforcement ratios
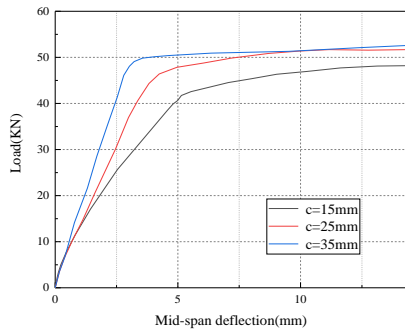
(c) load-deflection curves of

different cover layer thicknesses

(d) load-deflection curves of

different fire sides

(e) load-deflection curves of different ratio of shear span to effective depth

Fig. 18 Variation of load-flexural capacity of beams under different parameters

Clearly, the flexural capacity of RC beams was significantly weakened after the fire exposure, and the weakening was more obvious with the prolonging of fire exposure time. After the fire exposure, the cover layer thickness directly decided the temperature at the bottom of the tensile reinforcement, and with the larger cover layer thickness, the temperature at the bottom of the steels was lower and the mechanical performance was higher, leading to higher bearing capacity. The ratio of longitudinal reinforcement also affected the bending bearing capacity, and a larger reinforcement

ratio led to a higher bearing capacity. Similarly, the difference in fire sides has a great influence on the bearing capacity of the beam. Compared with the three-sided fire beam, the four-sided fire beam will damage the concrete in the compression zone, resulting in a reduction in the bearing capacity. The ratio of shear span to effective depth has little effect on the residual flexural capacity of the beam after fire.

6. Calculation method for residual flexural capacity of the RC beams

During the fire, the section temperature is unevenly distributed along the section height, so the distribution of concrete compressive strength after fire is not uniform throughout the section. To calculate the residual flexural capacity of the component after fire, the 500 °C isotherm method is adopted in Eurocode (BSI 2004). Han et al. (2007), Xiang et al. (2010) and Yang et al. (2002) used the equivalent section method to determine the ultimate flexural capacity of the beam under fire. This paper propose a new calculation model based on the FEA results and the improved section method to calculate the residual flexural capacity of the post-fire RC beams aiming at refining the flexural capacity calculation with the accurate inclusion of defects of strength reduction of the components caused by fire.

6.1 Basic assumptions

Before the calculation, the following basic assumptions are made for the RC beams after fire:

(1) The concrete strength of each grid in the compression zone was different, but the strength within each grid was considered as the same;

(2) The contribution of concrete in the tension zone to the residual flexural capacity was ignored;

(3) There was no relative slip between steel and concrete during the fire;

(4) The effect of temperature stress on the strength of the concrete at high temperature was not considered.

6.2 The limitation of this method

1) Ignore the effect of fine-tuning the cross-sectional size of the beam on the bending capacity of the beam.

2) it may require longer time period to predict flexural capacity than the existing

3) 500 °C isotherm method from Eurocode

6.3 Calculation steps

The beam section is meshed. The temperature of each cell can be extracted by the post-processing function of the ABAQUS from thermal analysis model. As shown in Fig.19, the temperature of concrete after the fire takes the highest temperature T_i in the i-th cell. The compressive strength reduction factor of concrete is obtained by substituting T_i into Equation 6. The temperature of the steel bar after the fire takes the highest temperature of the cell where the steel is located. The equation (12) for the yield strength of the steel bar after high temperature is adopted.

According to the strength reduction model of the concrete after high temperature in Fig.14, the post-fire residual flexural capacity is determined using the improved section method. The height of the compressive zone (x_c) of the concrete beam section after the fire can be calculated based on Equation (13):

$$f_c \sum \Psi_{cTi} \Delta b \Delta x + \Psi'_{yT} f'_y A'_s = \Psi_{yT} f_y A_s \qquad (13)$$

Where Ψ_{cTi} is the compressive strength reduction factor of the i-th cell, Δb is the width of a single cell, Δx is the height of a single cell, Ψ'_{yT} is the yield strength reduction factor of compressive steel, f'_y is the yield strength of compressive steel at room temperature, N/mm², A'_s and A_s is the area of steel in the compressive and tensile zone respectively, mm².
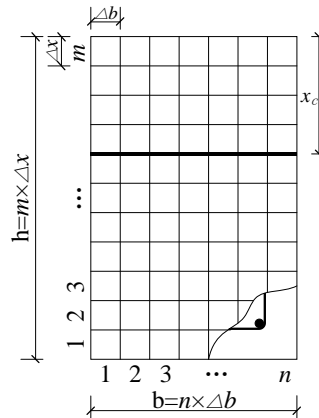
Fig. 19 Section unit division of beam

The strength reduction factor of concrete in the compressive zone ($\overline{\varPsi}_{cT}$) is obtained from the equation (14).

$$\overline{\varPsi}_{cT} = \frac{\sum \varPsi_{cTi} \Delta b \Delta x}{b x_c} \tag{14}$$

where b is the width of the beam section, x_c is the height of the compression zone of the concrete beam section.

After obtaining the height of the compression zone (x_c), the residual flexural capcity(M_u) of the RC beams after fire can be obtained according to equation (15).

$$M_u = \alpha_1 \overline{\varPsi}_{cT} f_c b x_c \left(h_0 - \frac{x_c}{2} \right) + \varPsi'_{yT} f'_y A'_s (h_0 - a'_s) \tag{15}$$

where α_1 is coefficient of equivalent rectangular stress figure in compression zone of concrete, which is 1 here, h_0 is the effective height of the beam section, a'_s is the distance from the resultant force point of the compressive steel reinforcement to the margins of the compressive section.

The flexural capacity of the RC beams after 60 minutes of fire is verified by the above theoretical method, and the flexural capacity after 90 minutes and 120 minutes of fire is calculated and compared with the finite element results. The results are shown in Fig. 20.
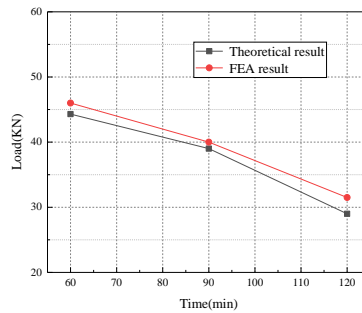
Fig. 20 Comparison of theoretical calculation and finite element calculation

6.4 Verification of the post-fire flexural capacity formula

The test data in Ref. (Xu et al. 2013) of specimen L5 is chosen to validate the correctness and applicability of the theoretical calculation model, and the dimensions and reinforcement of L5 beam

is illustrated in Fig. 21. The paper selects temperature measuring point 1# for verification. After the temperature field is simulated using ABAQUS, the nephogram of temperature field is shown in Fig. 22. The comparison between the simulation results and the test results of the Temperature-Time curve of measuring point 1# is shown in Fig. 23.
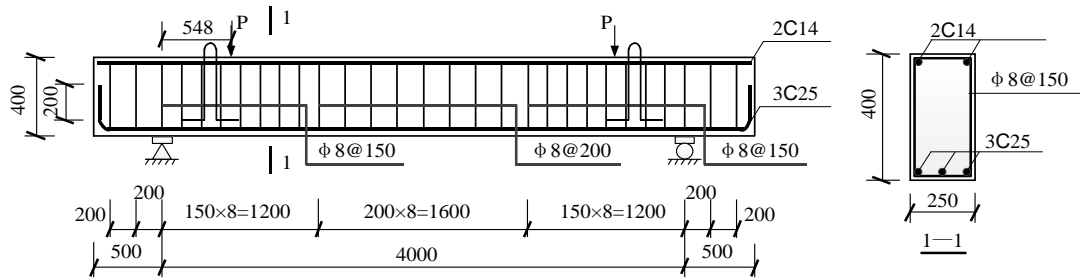

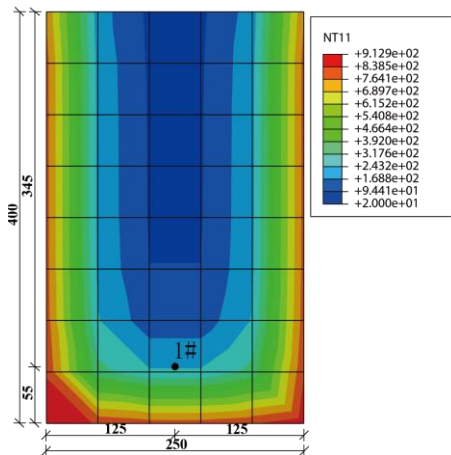**Fig. 21 The dimensions and reinforcement of L5 beam**

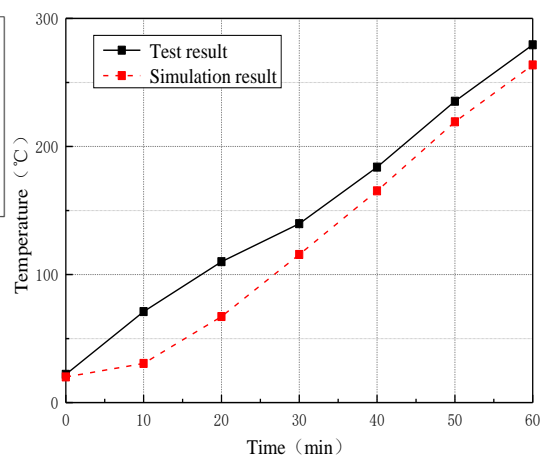**Fig. 22 The nephogram of temperature field of**

Fig. 23 The temperature-time curve of point 1#

L5 beam after 1 h of fire exposure

In order to more comprehensively compared the accuracy of the improved section method, the 500 ℃ isotherm method from Eurocode (BSI 2004) is now used to calculate the L5 beam. For a rectangular beam exposed to fire on three-sided, the schematic diagram of effective section of the beam is shown in Figure 24. In fact, the 500 ℃ isotherm method is a rough calculation method for the residual flexural capacity of the beam after fire. It is based on the assumption that concrete outside 500 ℃ no longer provides the bearing capacity of the member, while the residual concrete maintains its initial values of strength and elastic modulus. On the basic of the above assumptions, after obtaining the 500 ℃ isotherm, then determine a new width b_{fi} and a new effective height d_{fi} of

the section by excluding the concrete outside the 500 °C isotherm. The rounded corners of isotherms can be regarded by approximating the real form of the isotherm to a rectangle or a square. Then determine the reduced strength of the reinforcement according to the temperature of reinforcing bars in the tension and compression zones. Finally, the bending capacity of the beam post fire can be obtained based on the reduction factor of materials and the formula of bending capacity.
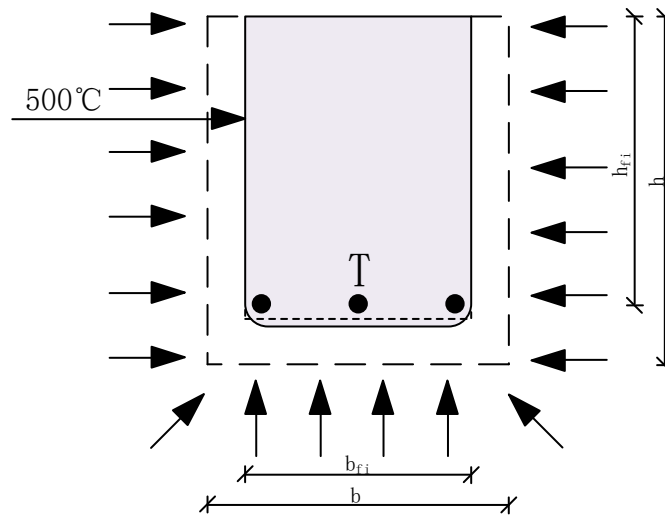
Fig. 24 Fire exposure on three sides with the tension zone exposed

According to the simulation method of the residual flexural capacity of the RC beam after fire in Section 4.3, after the simulation of the temperature field of the L5 beam subjected to fire for 60 minutes, the residual flexural capacity of the L5 beam is now simulated and compared with source test data. The results are shown in Fig. 25. The residual flexural capacity of the L5 beam of the test results of the improved section method results of the simulation results of the 500℃ isotherm method results are summarized in Table 4.
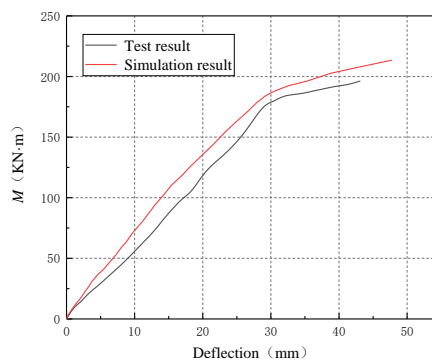
Fig. 25 The residual flexural capacity of the L5 beam after 1 h of fire exposure

Table 4   The results of the residual flexural capacity of the L5 beam after 1 h of fire exposure

Method	Result (KN·m)	Error (%)
Test	196	—
Simulation	201	2.55
500 ℃ isotherm	176.77	9.81
Improved section	194.45	0.79

The compressive strength reduction factor and the yield strength reduction factor of the section of beam after fire is determined according to Fig. 14 and Fig. 15. The flexural capacity of specimen L5 was calculated with Eq. (13-15) to be 194.45kN·m, with error 0.79% from that (196kN·m) of specimen L5 in Ref. (Xu et al. 2013) and was calculated with 500 ℃ isotherm method to be 176.77kN·m with error 9.81%. The flexural capacity of the theoretical calculation model proposed in this paper is well fitted with the Ref. (Xu et al. 2013), which indicates that the method can be applied accurately and effectively to the calculation of the flexural capacity of RC beams after fire.

7. Conclusions

The flexural capability of reinforced concrete after fire exposure was simulated on the finite element analysis software. The proposed theoretical calculation model based on improved section method and EFA was calculated and verified. The following conclusions can be drawn from the above research results.

1. The RC beams can be accurately simulated using the sequential thermo-mechanical coupling model developed in ABAQUS.

2. The fire exposure significantly weakened the flexural capacity and increase the deflection after a longer time of fire exposure.

3. Among the influence factors, the cover thickness, time of fire exposure, the ratio of longitudinal reinforcement, and the ratio of shear span to effective depth all largely

affected the flexural capacity of RC beams after fire exposure. The flexural capacity was enhanced with larger cover layer thickness or higher reinforcement ratio but reduced after longer time of fire exposure. The flexural capacity was severely weakened after four-sided fire. The ratio of shear span to effective depth has little effect on the residual flexural capacity of the beam after fire.

4. The flexural capacity of the post-fire beam obtained by the improved section method was consistent with the results obtained by the FEA software, and it was consistent with the experimental data, and the accuracy was high compared to other methods, which provided reference for the calculation of flexural capacity of RC beams after fire.

Acknowledgements

Authors' contributions

BC and FF designed the research methodology; BL performed the analysis, BL and FF draft the manuscript; BC and FF reviewed the manuscript. All authors read and approved the final manuscript.

Funding

Availability of data and materials

The data used to support the findings of this study are available from the authors upon request.

Competing interests

The authors declare that they have no competing interests.

Author information

Bin Cai,Professor, School of Civil Engineering, Jilin Jianzhu University, Changchun, China; School of Mathematics, Computer Science and Engineering, City, University of London, London, UK. Email :bincai666@163.com

Bo Li,Research student, School of Civil Engineering, Jilin Jianzhu University, Changchun, China.

Feng Fu, Senior Lecturer (Associate Professor), School of Mathematics, Computer Science & Engineering, Department of Civil Engineering, Northampton Square, London, C1V 0HB, U.K.(corresponding author). Email: feng.fu.1@city.ac.uk

References

Ban, D. L. (2008). Research on Building Fire Collapse. *Science and Technology Innovation Herald.* (26), 169-170.

Bratina, S., Planinc, I., Saje, M., & Turk, G. (2003). Non-linear fire-resistance analysis of reinforced concrete beams. *Structural Engineering and mechanics.* 16(6), 695-712.

BS 5950-8:2003 (Superseded, Withdrawn) Structural use of steelwork in building. Code of practice for fire resistant design

BSI. (2004). BS EN 1992-1-2: 2004, Eurocode 2—Design of concrete structures-part 1–2: General rules-structural fire design. Structural fire design. London: BSI.

Chen, Y. H., Chang, Y. F., Yao, G. C., & Sheu, M. S. (2009). Experimental research on post-fire behaviour of reinforced concrete columns. *Fire safety journal*, 44(5), 741-748.

Cheng, S. P., (2007). *Finite element analysis of temperature field and temperature stress of concrete structure*. Doctoral dissertation. Chongqing University.

Di Capua, D., & Mari, A. R. (2007). Nonlinear analysis of reinforced concrete cross-sections exposed to fire. *Fire Safety Journal*, 42(2), 139-149.

Eamon, C. D., & Jensen, E. (2013). Reliability analysis of reinforced concrete columns exposed to fire. *Fire safety journal*, 62, 221-229.

El-Hawary, M. M., Ragab, A. M., El-Azim, A. A., & Elibiari, S. (1997). Effect of fire on shear behaviour of RC beams. *Computers & Structures*, 65(2), 281-287.

Fu F., (2016 b) Structural Analysis and Design to Prevent Disproportionate Collapse, CRC Press ISBN 978-1-4987-8820-5

Fu, C. G., Liu, W., & Kong, W. Y., & Wang, Y. Z. (2015). The temperature field analysis of reinforced concrete beam based on heating and cooling whole curve. *Journal of Shandong Jianzhu University*, 30(4), 307-317.

Fu, F. (2012). Response of a multi-storey steel composite building with concentric bracing under consecutive column removal scenarios. Journal of Constructional Steel Research, 70, pp. 115–126

Fu, F. (2016a). 3D finite element analysis of the whole-building behavior of tall building in fire. Advances in Computational Design, 1(4), pp. 329–344.

Fu, F. (2020). Fire induced progressive collapse potential assessment of steel framed buildings using machine learning. Journal of Constructional Steel Research, 166, pp. 105918–105918

Fu, F.(2018). Design and Analysis of Tall and Complex Structures. Butterworth-Heinemann, ELSEVIER, ISBN 978-0-08-101121-8.

Fu, F., Lam, D. and Ye, J. (2008). Modelling semi-rigid composite joints with precast hollowcore slabs in hogging moment region. Journal of Constructional Steel Research, 64(12), pp. 1408–1419.

Fu, F., Lam, D. and Ye, J. (2010). Moment resistance and rotation capacity of semi-rigid composite connections with precast hollowcore slabs. Journal of Constructional Steel Research, 66(3), pp. 452–461

Han, Y. L., Wang, Z. Q., Wang, Y. J., & Bai, L. L.(2007). Analysis of bending capability of a reinforced concrete beam supported at both ends in fired field. *Journal of Naval University of Engineering*, 19(1), 76-80.

Hassan, A., Aldhafairi, F., Abd-EL-Hafez, L. M., & Abouelezz, A. E. Y. (2019). Retrofitting of different types of reinforced concrete beams after exposed to elevated temperature. *Engineering Structures*, 194, 420-430.

Hu, C. P., Xu, Y. Y., Luo, Y., Zheng, Y. L., & Lin, B. L. (2014). Experimental study on the tensile strength of concrete after high temperature. *Journal of Huaqiao University (Natural Science)* 35(2), 196-201.

Hu, Q., Xu, M. X., Zheng, W. Z. (2006). Estimation method for normal section load-flexural capacityof concrete members subjected to fire. *Journal of Harbin Institute of Technology*, 38(1), 56-58.

ISO (International Organisation for Standardisation) (1999) ISO 834-1: Fire resistance tests-Elements of building construction. Part 1: general requirements. Geneva: ISO.

Jiang, F. G., Chen, H., Bai, L. L. (2008). Analysis and calculation of residual bearing capacity of

Kodur, V. K. R., & Agrawal, A. (2017). Effect of temperature induced bond degradation on fire response of reinforced concrete beams. *Engineering Structures*, 142, 98-109.

Liao, J. H., Lu, Z. D., & Su, L. (2013). Experimental and Finite Element Analysis of Shear Strength of Concrete Beams Subjected to Elevated Temperature. *Journal of Tongji University (Nature Science)* 41(6), 806-812.

Lie, T. T., & Irwin, R. J.. (1993). Method to calculate the fire resistance of reinforced concrete columns with rectangular cross section. *aci structural journal,* 90(1), 52-60.

Lu, Z. D., Zhu, B. L., & Zhou, Y. H. (1993). Experimental study on fire response of simple supported reinforced concrete beams. *China Civil Engineering Journal* 26(3), 47-54.

Mathew, G., & Joseph, B. (2018). Flexural behaviour of geopolymer concrete beams exposed to elevated temperatures. *Journal of Building Engineering*, 15, 311-317.

Miao, J. J., Chen, N., Hou, X. Y., Zhu, Q. Q., & Gong, W. (2013). Experimental research and numerical simulation on fire resistance performance of RC beams with damages caused by service loading. *Journal of Building Structures*, 34(03), 1-11.

Parthasarathi, N., Saraf, D. S., Prakash, M., & Satyanarayanan, K. S. (2019). Analytical and Experimental study of the reinforced concrete specimen under elevated temperature. *Materials Today: Proceedings*, 14, 195-201.

reinforced concrete beams after fire. Concrete, 000(002), 57-59.

Shao, H. Y., Zhu, R. X., & Ren, C. X., (2003). Finite element analysis of temperature field and temperature stress field of structure. *Journal of Ningbo University (Nature Science & Engineering),* 16(1), 57-60.

Shi, X. D., & Guo, Z. H. (2000). Investigation on the behavior of reinforced concrete at elevated temperature. *China Civil Engineering Journal* 33(6), 6-16.

Sun, J. F., Shi, X. D., & Guo, Z. H. (2002). Experimental study on the mechanical behavior of three-sided heated reinforced concrete beams at high temperature and after cooling. *Building Structure* 32(1), 34-36.

Tian, M. G, (2002). *Research and application of damage assessment of reinforced concrete structure after fire*. Doctoral dissertation. Hunan University.

Wang, Z. Q., & He, J. (2009). *Nonlinear analysis of reinforced concrete structures*. Harbin：Harbin Institute of Technology Press.

Xiang, K., Wang, G. H., Yu, J. T., Wang, S., & Diao, X. L. (2010). Uniform calculating method of flexural capacity for fire-damaged reinforced concrete bending members. *Fire Science and Technology*, 29(12), 1035-1039.

Xu, Q., Han, C., Wang, Y. C., Li X., Chen, L., & Liu, Q. (2015). Experimental and numerical investigations of fire resistance of continuous high strength steel reinforced concrete T-beams. *Fire Safety Journal*, 78, 142-154.

Xu, Y. Y., Wu, B., Wang, R. H., Jiang, M., & Luo, Y. (2013). Experimental study on residual performance of reinforced concrete beams after fre. *Journal of Building Structures, 34*(8), 20–29.

Yang, J. P., Shi, X. D., & Guo, Z. H. (2002). Simplified calculation of ultimate load flexural capcityof reinforced concrete beams under high temperature. *Industrial Construction*, 32(3), 26-28.

Yu, Z. W., Ding, F. X., & Luo, J. P. (2005). Experimental research on mechanical properties of different type of concrete after high temperature. *Journal of Safety and Environment*, 5(5), 1-6.

Yu, Z. W., Wang, Z. Q., & Shi, Z. F. (2005). Experimental research on material properties of new three-grade steel bars after fire. *Journal of Building Structures*, 26(02), 112-116.

Zeng, Y. F, (2006). *Study on damage assessment and identification of reinforced concrete structure after fire*. Doctoral dissertation. Chongqing University.

Zhao, M. M, (2014). *Discussion on temperature stress characteristics of concrete*. Doctoral dissertation. Tianjin University.